

Correlation Driven Topological Insulator-to-Weyl Semimetal Transition in Actinide System UNiSn

Vsevolod Ivanov[†], Xiangang Wan^{*}, Sergey Y. Savrasov[†]

[†]*Department of Physics, University of California, Davis, CA 95616, USA and*

^{*}*Department of Physics, Nanjing University, Nanjing 210093, China*

(Dated: November 22, 2021)

Although strong electronic correlations are known to be responsible for some highly unusual behaviors of solids such as, metal-insulator transitions, magnetism and even high-temperature superconductivity, their interplay with recently discovered topological states of matter awaits full exploration. Here we use a modern electronic structure method combining density functional theory of band electrons with dynamical self-energies of strongly correlated states to predict that two well-known phases of actinide compound UNiSn, a paramagnetic semiconducting and antiferromagnetic metallic, correspond to Topological Insulator (TI) and Weyl semimetal (WSM) phases of topological quantum matter. Thus, the famous unconventional insulator-metal transition observed in UNiSn is also a TI-to-WSM transition. Driven by a strong hybridization between U f-electron multiplet transitions and band electrons, multiple energy gaps open up in the single-particle spectrum whose topological physics is revealed using the calculation of Z_2 invariants in the strongly correlated regime. A simplified physical picture of these phenomena is provided based on a periodic Anderson model of strong correlations and multiple band inversions that occur in this fascinating compound. Studying the topology of interacting electrons reveals interesting opportunities for finding new exotic phase transitions in strongly correlated systems.

PACS numbers:

Here we argue that an unusual phase transition at $T_N=43\text{K}$ between a higher temperature paramagnetic semiconducting (P-S) and low temperature antiferromagnetic metallic (AFM) phase discovered in the past [1] for a strongly correlated actinide system UNiSn, simultaneously corresponds to the transition between two topological phases of quantum matter, Topological Insulator (TI) and Weyl semimetal (WSM), that have recently received a great interest due to the appearance of robust electronic states insensitive to perturbations[2, 3]. This actinide compound has been extensively studied during last several decades owing to its unconventional (inverse) nature of this metal-insulator transition with the gap opening above T_N and associated behavior of its strongly correlated 5f electrons. It crystallizes in a cubic structure (MgAgAs-type) (see Fig. 1a) and its paramagnetic semiconducting phase has an estimated energy gap of about 100 meV [4]. Its antiferromagnetic structure was found to be of type I with the ordered U moment $1.55 \mu_B$ oriented along the (001) axis [1].

The central issue in understanding the physical properties of actinides is the degree to which their 5f electrons are localized. Due to the absence of any signatures of heavy fermion behavior in the specific heat data[4], the magnetic behavior of UNiSn has been explained [5] on the basis of a localized $5f^2$ (U^{4+}) ionic state, whose ground state multiplet 3H_4 ($J=4$) subjected to a cubic crystal field is split into a doublet (Γ_3), two triplets (Γ_4, Γ_5) and a singlet (Γ_1). Measured temperature-dependent susceptibility and magnetic entropy analysis suggested that the non-magnetic doublet is the lowest lying state 180K below the Γ_4 triplet and 430 K below the Γ_1 singlet (see Fig.

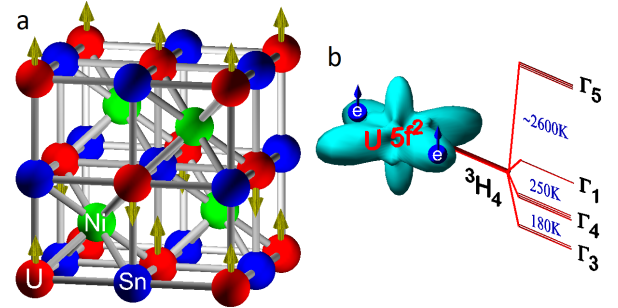


FIG. 1: a. Crystal structure of UNiSn showing antiferromagnetic type I ordering [1], b. Effect of the cubic crystal field splitting on the 3H_4 ground state multiplet of the U f^2 two-electron state with its lowest non-magnetic Γ_3 doublet as found experimentally[5].

1b). Since Γ_3 has a quadrupole moment, it was further proposed that tetragonal distortions and quadrupolar ordering exists below T_N [1]. The valence band photoemission spectra revealed a dominant 5f electron character for the states in the vicinity of the Fermi level with a contribution from U 6d, Ni 3d and Sn 6p states [6].

Previous band structure calculations of UNiSn emphasized the role of relativistic effects and electronic correlations among 5f electrons [7]. Both P-S and AFM behavior have been captured correctly within the LDA+U framework[8], where on-site Coulomb correlations among f electrons are treated via the introduction of the Hubbard U term and subsequent static mean field approximation. Such a method is expected to work well in a symmetry broken AFM state, but would be invalid for the gen-

uine two–electron Γ_3 doublet represented by a mixture of Slater determinants. One can however, assume that paramagnetism originates from the non–magnetic Γ_1 singlet, for which LDA+U should be sufficient. Within a single–particle picture this is interpreted as a doubly occupied Γ_7 level that appears when a 14 fold degenerate manifold of 5f electrons subjected to spin–orbit coupling and cubic crystal field is split into Γ_7, Γ_8 (for $j=5/2$) and $\Gamma_6, \Gamma_7, \Gamma_8$ (for $j=7/2$) sublevels. Detailed comparisons between theory and experiment revealed discrepancies in the position of the occupied f–band with respect to the Fermi energy: -0.3 eV in the photoemission vs. -1 eV in the LDA+U calculation[6].

Nowadays, modern electronic structure approaches based on combinations of local density approximation and dynamical mean field theory (so called LDA+DMFT) [9] are free from these difficulties, and allow for a more accurate treatment of Coulomb interactions in UNiSn via computations of local self–energies $\Sigma(\omega)$ for the interacting 5f electrons. This is achieved by treating a correlated 5f shell as an impurity hybridized with the non–interacting bath which is then periodized and subjected to self–consistency. An exact solution of such an Anderson impurity problem is possible in principle via a recently developed Continuous Time Quantum Monte Carlo (CT–QMC) method [10], although accounting for the full Hilbert space of interacting f electrons together with spin–orbit and crystal field terms represents a challenge. In addition, the CT–QMC works on the imaginary time–frequency axis and obtaining frequency dependence of the self–energy on the real axis involves an analytical continuation algorithm which is known to be not very accurate.

In order to study the topology of correlated electrons in UNiSn here we take a pragmatic approach and make the problem numerically tractable by using the experimental fact that the Uranium f electrons are localized in their $5f^2 \Gamma_3$ ground state, from which the one–electron multiplet transitions can be obtained by exact diagonalization. The corresponding f–electron self–energies are subsequently expanded in the Laurent series which allows us to replace the non–linear (in energy) Dyson equation by a linear Schroedinger–like equation in an extended subset of “pole states” [11]. Remarkably, the pole representation for the self–energy results in the appearance of many–body satellites and multiplets in the spectra as effective band states, in general carrying a fractional occupancy due to the spectral weight transfer. It is ideally suited for studying topological indices as the corresponding auxiliary wave functions representing the many–body features carry all necessary information about the Berry phase of the interacting electrons[12].

We now present the results of our calculation for the paramagnetic phase of UNiSn which is carried out by treating f–electrons in their $5f^2 \Gamma_3$ ground state. The Coulomb interaction matrix elements needed for the

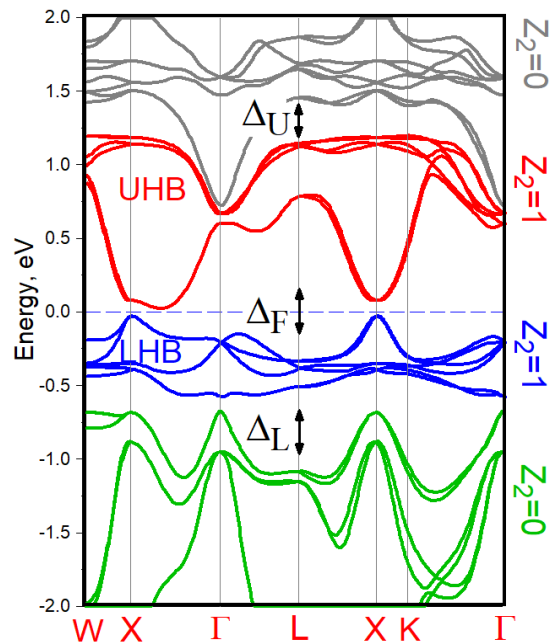


FIG. 2: Calculated electronic structure of UNiSn using density functional theory combined with dynamical self–energies for the Uranium f–electrons assuming experimentally determined $5f^2 \Gamma_3$ doublet as a ground state[5], The locations of energy panels with non–zero Z_2 invariants and corresponding gaps ($\Delta_L, \Delta_F, \Delta_U$) are indicated.

exact diagonalization procedure ($F^{(0)}, F^{(2)}, F^{(4)}, F^{(6)}$ Slater integrals) have been found from the atomic 5f–electron wave functions and scaled to account for screening effects. We cover a range of these parameters: 2–4 eV for the Hubbard $U = F^{(0)}$ and 0–1 eV for the exchange $J = (286F^{(2)} + 195F^{(4)} + 250F^{(6)})/6435$, in order to make sure that our conclusions are not altered by the lack of an accurate procedure for determining the screening. It has been argued earlier that these values are typical for obtaining the best agreement between theory and experiment for several Uranium compounds [6, 7]. The position of the bare f–level is fixed by reproducing the experimentally observed $f^2 \rightarrow f^1$ electron removal transition at -0.3 eV [6]. The charge density self–consistency is carried out within the LDA+DMFT as implemented by one us earlier[13].

Fig. 2 shows our calculated many–body electronic spectrum in the vicinity of the Fermi level using a set of Slater integrals $F^{(0)} = 0.15, F^{(2)} = 0.3, F^{(4)} = 0.2, F^{(6)} = 0.15$ in Rydberg units. Although cast into a conventional band structure plot, we stress that the 5f electron states are treated here as true one–electron removal ($f^2 \rightarrow f^1$) and addition ($f^2 \rightarrow f^3$) processes that come from exact diagonalization, and corresponding “energy bands” carry non–integer occupation. This can be seen by realizing that the multiplet transitions within the $j = 5/2$ manifold (shown in this Figure by red and blue)

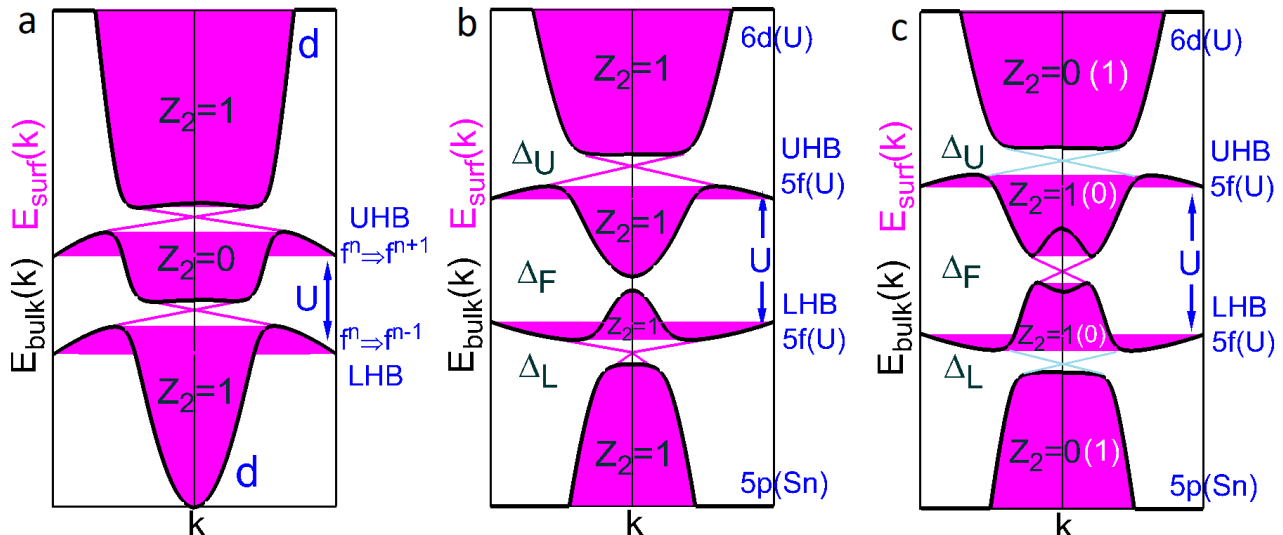


FIG. 3: Band inversion mechanism applicable for UNiSn: a. In the periodic Anderson model, hybridization between a wide d-band and f-electron multiplet transitions (lower and upper Hubbard bands, LHB and UHB) results in three energy panels (shown by black lines) and two gaps that are both topologically non-trivial. The corresponding surface spectrum is shown by magenta color, where the spectral weight of the Dirac cone is distributed between the two gaps. b. In UNiSn, the upper Hubbard band is inverted with the wide 6d band of Uranium while the lower Hubbard band is inverted with the 5p band of Tin, resulting in four energy panels and three gaps. With two such band inversions, upper, Δ_U , and lower, Δ_L , the hybridization gaps are topological while the fundamental bulk gap, Δ_F , is not. c. The band inversion between U 6d and Sn 5p states makes the fundamental gap Δ_F topological. The topological features of the gaps Δ_U, Δ_L are seen to disappear in the LDA+DMFT calculation, but this is not a requirement within the considered model (Z_2 invariants shown in parentheses are expected).

are represented by 6 energy bands that appear both below and above the Fermi level. These are the famous lower and upper Hubbard bands within the Mott gap picture that acquire a significant dispersion due to hybridization with U 6d and Sn 5p orbitals. The deduced value of the indirect energy gap shows some dependence on the Slater integrals, but falls into the same range as experiment (~ 100 meV [4]).

We now turn to the prediction of topological properties of the paramagnetic semiconducting phase of UNiSn. First, we point out that the underlying crystal structure is not centro-symmetric, therefore the Fu and Kane parity criterion[14] developed for insulators with both time reversal and inversion symmetries does not apply. Nevertheless, given the fact that the Uranium sites arrange themselves in the inversion symmetric face centered cubic sublattice with their odd parity localized 5f electrons lying in close proximity to the Fermi level, it is interesting to speculate whether the possibility of inversion with the even parity U 6d band is taking place. Such an f-d band inversion was at the center of recent interest for several topological Kondo insulator materials with 4f electrons[15], as well as in some actinide systems such as AmC[16]. While the U 6d band is expected to be unoccupied, it is very wide, with its lower portion hybridized with the Hubbard bands. The Fu and Kane criterion would then imply the existence of topological Dirac cone

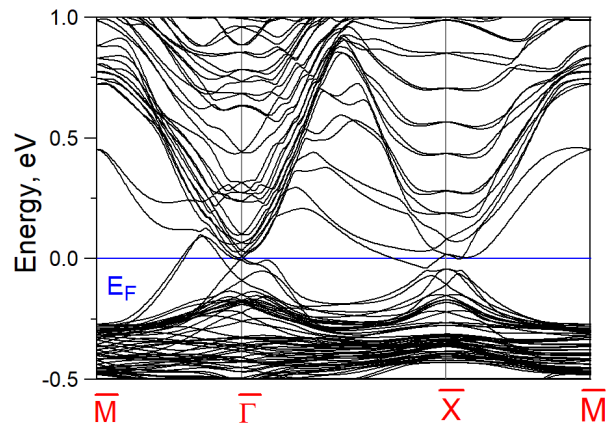


FIG. 4: Surface spectrum of UNiSn calculated using LDA+DMFT method, assuming a $5f^2 \Gamma_3$ doublet as a ground state. The fundamental energy gap shows topological Dirac cone dispersions in the vicinity of the $\bar{\Gamma}$ and \bar{X} points.

states in UNiSn.

To uncover the topological physics one needs to compute Z_2 invariants [17] for the occupied band manifold in the difficult regime of strong correlations. Fortunately, it was recently proved that utilizing a pole representation for the self-energy[11], reduces this problem to an effective non-interacting system in the extended set of pole states, whose topological indices are exactly matched

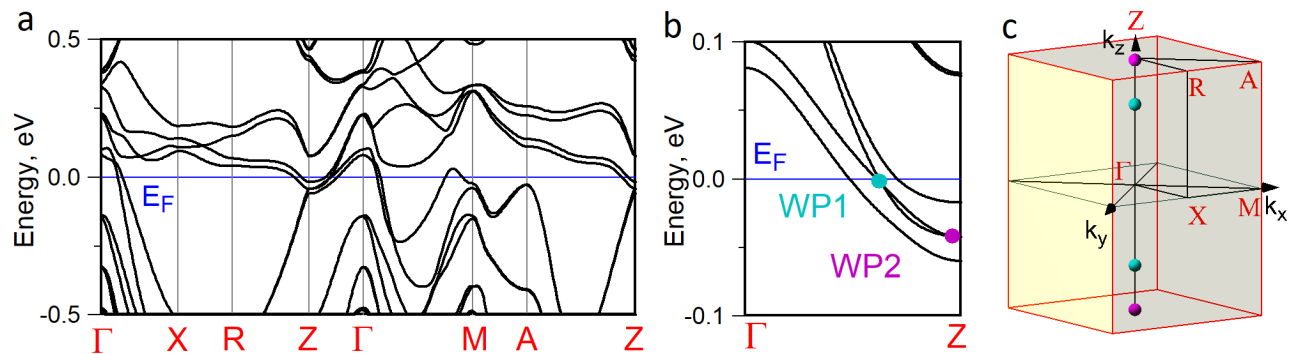


FIG. 5: Calculations for antiferromagnetic configuration of UNiSn. a. Energy band dispersions along major high symmetry lines of the Brillouin Zone, b. Zoomed area along the ΓZ direction of the BZ showing the locations of the Weyl points, c. Brillouin Zone of the AFM UNiSn with the positions of the Weyl points.

[12]. We develop and carry out this computation within the n -field approach[18]. However, some care should be taken to define an appropriate energy panel because as it is seen from our calculations that multiple gaps appear in the excitational spectrum of UNiSn (we show the panels by various colors and denote the gaps between them as $\Delta_L, \Delta_F, \Delta_U$ in Fig. 2). For example, six dispersive features that represent the lower Hubbard bands (blue colored "spaghetti" in Fig. 2 labeled as LHB) are completely gapped from the remaining band manifold everywhere in the BZ. The same is seen for the six eigenstates representing the upper Hubbard bands above the E_F (red colored "spaghetti" in Fig. 2 labeled as UHB). Our computations of Z_2 invariants for the four energy panels separated by $\Delta_L, \Delta_F, \Delta_U$ reveal their topological indices that we indicate on the right margin in Fig. 2. The energy panels below and above the fundamental gap correspond to the indices equal to 1;(000) in the notations of Ref. [17] (we denote this result by $Z_2 = 1$ in Fig. 2). This suggests that UNiSn is a strong topological insulator and prompts on the existence of protected Dirac cone states at its surface.

To understand which orbitals are responsible for the appearance of the topological phase, we carry out calculations using a constrained hybridization approach[19]. In this method, the energies of particular orbitals are shifted by applying a constant potential constrained within the orbital space by projector operators. This is similar to the LDA+U, LDA+DMFT and other families of methods that combine the self-energy with LDA (SELDA family [20]), restricting the application of the self-energy to the subspace of correlated orbitals. Utilizing this procedure, we are able to de-hybridize various states, such as U-5f, U-6d, Ni-3d, Sn-5p, etc., by shifting their energies away from the relevant energy window, and recompute Z_2 invariants. The outcome of this study is the existence of multiple band inversions in UNiSn: The upper Hubbard band is inverted with the U 6d electrons, the lower Hubbard band is inverted with Sn 5p electrons, and, most

importantly, U 6d electrons at the very bottom of the conduction band and Sn 5p states at the very top of the valence band are also inverted around the X point of the BZ (see Fig. 2). This band inversion is responsible for the topological insulator property of UNiSn.

To illustrate the emergent physical picture, we use the periodic Anderson model (PAM) of strong correlations. It has been recently employed for developing the concept of topological Kondo insulators where the Fermi level falls into the gap between a heavy fermion (f -like) and non-interacting (d -like) bands[15]. It has also been recently used to describe Weyl-Kondo semimetals via hybridization of a heavy-fermion state with non-interacting bands containing the nodal points[21]. In our case the f -electrons are localized and their self-energies behave similarly to the famous Hubbard I approximation: $\Sigma(\omega) = U^2/4\omega$. The solution of the PAM in this limit is schematically illustrated in Fig. 3a. Hybridization between a wide d -band and f -electron multiplet transitions denoted as LHB and UHB results in the appearance of two gaps in the spectrum and three energy panels (shown by black lines). Both gaps are seen to be topologically non-trivial due to the d - f band inversion mechanism. For a centrosymmetric lattice, this can be understood based on the Fu and Kane parity criterion [14]: for the lower (upper) panel, the parities of the eigenstates are odd (even) at BZ boundary time reversal invariant momenta (TRIM), such as the X and L points of cubic BZ, but even (odd) at Γ . This results in the energy gap above (below) the panel to be topological. For the central panel, the parities of the eigenstates are odd everywhere, but this does not preclude having topological gaps below and above the panel, each with its own Dirac cone (the total number of cones is even). We illustrate the corresponding surface spectrum by magenta color. Note that since the Hubbard bands carry no integer occupation, the spectral weight of the Dirac cones is also re-distributed between the two gaps.

Now, in UNiSn, our constrained hybridization proce-

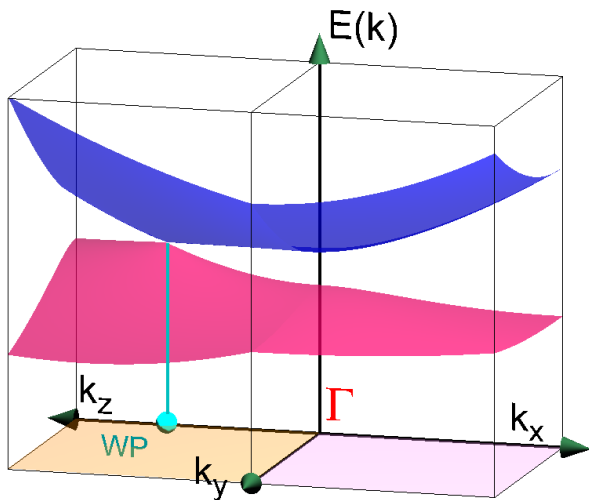


FIG. 6: Dispersion of two intermediate eigenstates of a 4×4 $k \cdot p$ model used to illustrate the magnetization induced Weyl semimetal state in UNiSn. The band structure is gapped for all k -points in the BZ except along the ΓZ line where the Weyl point is formed.

ture reveals multiple band inversions: First, as illustrated in 3b, the upper Hubbard band is inverted with the U 6d, while the lower Hubbard band is inverted with Sn 5p. Due to the d-f band inversion, the topological Dirac cone is expected to appear inside the gap Δ_U at the surface spectrum. Since Uranium atoms occupy sites of the centrosymmetric face centered cubic lattice, this can be understood based on the parity criterion [14]. For the lower Hubbard band, U 5f and Sn 5p orbitals are both odd, but they occupy different sites (forming a diamond-like lattice) where the inversion center can be imagined approximately in the middle between the atoms. Such model will also produce a strong topological insulator (the Dirac cone is inside the gap Δ_L) provided that the irreducible representations of the U 5f and Sn 5p orbitals are different, e.g. Γ_7 and Γ_6 . This picture emerges when the bottom of the U 6d and the top of Sn 5p bands are not inverted around the X point, making the fundamental gap Δ_F not topological, as we show in 3b. Realizing the band inversion between the U 6d and Sn 5p bands at the X point (see Fig. 3c) results in the fundamental gap Δ_F becoming topological. Additionally, we monitor the cancellation of the topological features inside the gaps Δ_U, Δ_L . This is apparently due to a more complex overlap between various orbitals in the real calculation than the one assumed in the simplified model illustrated in Fig. 3c where one would in principle expect all three gaps to become topological ($Z_2 = 0$ for the LHB and UHB, and $Z_2 = 1$ for the lowermost and topmost panels as shown in brackets in Fig. 3c).

To verify these conclusions, we additionally carry out the charge density self-consistent LDA+DMFT calcula-

tion of the surface one-electron spectrum. We construct a slab spanned along z direction and terminated by U plane from the top and by Ni plane from the bottom. The slab sizes are varied between 4 and 8 unit cells and the distance between the slabs is set to 14 Å to ensure the convergence of the surface states. The results are shown in Fig. 4. We clearly resolve the Dirac cone states inside the fundamental energy gap Δ_F of UNiSn that appear around the Γ of the surface BZ. There are also Dirac cone-like features around the \bar{X} point. It is interesting to note that there are other surface states propagating across the gap and hybridizing with the Dirac cones. This makes the Dirac cone dispersions appear within small areas around the TRIM points, but break apart at higher momenta.

We now turn to discussing the results of our calculation for the low temperature AFM phase of UNiSn. The origin of magnetism has been explained earlier [5] based on a molecular-field model, where owing to the second-order effect in the magnetic exchange field, the Γ_3 doublet is split into two levels with the deduced value of magnetic moment $\sim 2.6\mu_B$. Here our exact diagonalization for the 5f states is almost identical to the static mean field solution, because the double degeneracy of Γ_3 is broken and a single Slater determinant description suffices. It has been also proven earlier that the LDA+DMFT method reduces to the LDA+U in the Hartree-Fock limit[22]. Our calculation with the Slater integrals $F^{(0)} = 0.15, F^{(2)} = 0.3, F^{(4)} = 0.2, F^{(6)} = 0.15$ in Rydberg units converges to an antiferromagnetic state with the total magnetic moment of $2.1\mu_B$ ($+3.2\mu_B$ for its orbital and $-1.1\mu_B$ for its spin counterparts) slightly larger than the experimentally deduced value of $1.55\mu_B$ [1]. This is in agreement with previous works [6, 7] that also pointed out the inclusion of spin fluctuations as a possible way to reduce these values. Our calculated spin density matrices resemble those obtained from the molecular-field exchange model [5].

Fig. 5a shows our calculated band structure along major high symmetry directions of the BZ. A few energy bands are seen to cross the Fermi level indicating the metallic nature of the solution. The most striking finding of our AFM calculation is however the existence of the Weyl points in close proximity to the Fermi level which appear exactly along the ΓZ line of the BZ, serving here as the magnetization direction. Since the Weyl points act as Dirac monopoles in k -space, we verify their precise locations by computing the Berry flux that originates from each point. The corresponding band structure is shown in Fig. 5b, which indicates that the Weyl points are of type II according to classification introduced in Ref. [23]. Fig. 5c shows the positions of these Weyl points in the Brillouin Zone. Negative magnetoresistance measurements have been reported for this compound [24] which can be an indication that the chiral anomaly characteristic for Weyl semimetals exists here.

To understand the physical origin behind magnetization induced Weyl state in UNiSn, we introduce a two

orbital $k \cdot p$ model for two relativistic orbitals with an inversion breaking term.

The Hamiltonian reads

$$H_{eff} = \begin{pmatrix} A(\mathbf{k}) + \Delta & 0 & Pk_z + iV_{k_x k_y} & Pk_- + Vk_z k_+ \\ 0 & A(\mathbf{k}) - \Delta & Pk_+ - Vk_z k_- & -Pk_z - iV_{k_x k_y} \\ Pk_z - iV_{k_x k_y} & Pk_- - Vk_z k_+ & B(\mathbf{k}) + \Delta & 0 \\ Pk_+ + Vk_z k_- & -Pk_z + iV_{k_x k_y} & 0 & B(\mathbf{k}) - \Delta \end{pmatrix} \quad (1)$$

where $k_{\pm} = k_x \pm ik_y$ and bands $A(\mathbf{k}) = A_0 + A_1 \mathbf{k}^2$, $B(\mathbf{k}) = B_0 + B_1 \mathbf{k}^2$ assume some quadratic (possibly different dispersion). The parameter P controls the inversion breaking. This model was previously used to describe topological insulator and Weyl semimetal phases in zincblende-like structures[25]. Here we apply a Zeeman splitting to each band A and B by setting the parameter $\Delta \neq 0$ along the magnetization (z) axis. Once the effective "spin up" and "spin down" states cross, they produce a Weyl point exactly along 001 direction in the BZ while the gap between these bands is open for all other \mathbf{k} -points provided the inversion breaking P term is non zero. We illustrate this behavior in Fig. 6 which shows the dispersion of two middle eigenvalues of Eq. 1, which are seen to produce the Weyl point along ΓZ . Note also that setting $P = 0$ will produce chiral nodal lines.

One of the most striking features of Weyl semimetals is the presence of the Fermi arcs in their one-electron surface spectra [26]. Although computations of their shapes are possible via a self-consistent supercell (slab) calculation of the surface energy bands, given the variety of regular Fermi states that emerge from our AFM calculation together with the fact that the Weyl points are not exactly pinned at the Fermi level, makes it hard to resolve them in the surface spectrum. Nevertheless, since the arcs connect the Weyl points of different chirality, one can expect the existence of long arc-like features in UNiSn that should be protected from perturbations such as disorder[27].

In conclusion, based on a computational approach combining density functional theory of electronic structure and dynamical mean field theory of strong correlations, we showed that two topological phases of quantum matter, topological insulator and Weyl semimetal, accompany the unconventional insulator-metal transition in the 5f electron compound UNiSn. We uncovered physical origin of its topological insulator behavior via the occurrence of multiple band inversions between localized f-electrons and regular band states. We also concluded that the magnetic ordering triggers the Weyl state with the nodal points appearing along the magnetization direction. Our study reveals interesting opportunities for finding other topological phase transitions in strongly

correlated systems. Of particular interest are some non-centrosymmetric actinide compounds where the interplay between delocalized band electrons and correlated f-states together with the large spin-orbit coupling is expected to provide a new playground for studying topological properties of interacting electrons.

The work was supported by NSF DMR Grant No. 1411336. X. G. Wan was supported by NSF of China, Grant No. 11525417.

-
- [1] T. Akazawa, T. Suzuki, F. Nakamura, T. Fujita, T. Takabatake, and H. Fujii, Anomalous Magnetic Transition in UNiSn, *J. Phys. Soc. Japan.* **65**, 3661-3665 (1996).
 - [2] For a review, see, e.g., M. Z. Hasan, C. L. Kane, Colloquium: Topological insulators, *Rev. Mod. Phys.* **82**, 3045 (2010).
 - [3] For a review, see, e.g., N.P. Armitage, E. J. Mele, A. Vishwanath, Weyl and Dirac Semimetals in Three Dimensional Solids, *Rev. Mod. Phys.* **90**, 15001 (2018).
 - [4] For a review, see, e.g., P. S. Riseborough, Heavy fermion semiconductors, *Advances in Physics* **49**, 257-320 (2000).
 - [5] Y. Aoki, T. Suzuki, T. Fujita, H. Kawanaka, T. Takabatake, and H. Fujii, *Phys. Rev. B* **47**, 15060 (1993).
 - [6] J.-S. Kang, J.-G. Park, K. A. McEwen, C. G. Olson, S. K. Kwon and B. I. Min, *Phys. Rev. B* **64**, 085101 (2001).
 - [7] P. M. Oppeneer, A. N. Yaresko, A. Ya. Perlov, V. N. Antonov, and H. Eschrig, Theory of the anomalous magnetic phase transition in UNiSn, *Phys. Rev. B* **54**, 3706-3709 (1996).
 - [8] For a review, see, e.g, Strong Correlations in electronic structure calculations, edited by V. I. Anisimov (Gordon and Breach Science Publishers, Amsterdam, 2000).
 - [9] For a review, see, e.g, G. Kotliar, S. Y. Savrasov, K. Haule, V. S. Oudovenko, O. Parcollet, C.A. Marianetti, *Rev. Mod. Phys.* **78**, 865-951, (2006).
 - [10] For a review, see, e.g., E. Gull, A. J. Millis, A. I. Lichtenstein, A. N. Rubtsov, M. Troyer, and P. Werner, *Rev. Mod. Phys.* **83**, 349 (2011).
 - [11] S. Y. Savrasov, K. Haule, and G. Kotliar, Many-Body Electronic Structure of Americum Metal, *Phys. Rev. Lett.* **96**, 036404 (2006).
 - [12] L. Wang, H. Jiang, X. Dai, and X. C. Xie, Pole expansion of self-energy and interaction effect for topological insulators, *Phys. Rev. B* **85**, 235135 (2012).
 - [13] S. Savrasov, G. Kotliar, and E. Abrahams, Electronic

- correlations in metallic Plutonium within dynamical mean-field picture, *Nature* **410**, 793 (2001).
- [14] L. Fu and C. L. Kane, Topological insulators with inversion symmetry, *Phys. Rev. B* **76**, 045302 (2007).
- [15] For a review, see, e.g., M. Dzero, J. Xia, V. Galitski, and P. Coleman, Topological Kondo Insulators, *Annu. Rev. Condens. Matter Phys.* **7**, 249-280 (2016).
- [16] X. Zhang, H. Zhang, J. Wang, C. Felser, S.-C. Zhang, Actinide Topological Insulator Materials with Strong Interaction, *Science* **335**, 1464 (2012).
- [17] C. L. Kane and E. J. Mele, Z_2 Topological Order and the Quantum Spin Hall Effect, *Phys. Rev. Lett.* **95**, 226801 (2005).
- [18] T. Fukui and Y. Hatsugai, Quantum Spin Hall Effect in Three Dimensional Materials: Lattice Computation of Z_2 Topological Invariants and Its Application to Bi and Sb, *Journal Phys. Soc. Japan* **76**, 053702 (2007).
- [19] X. Wan, J. Zhou and J. Dong, The electronic structures and magnetic properties of perovskite ruthenates from constrained orbital-hybridization calculations, *EPL* **92**, 57007 (2010).
- [20] For recent applications of SELDA, see, e.g., S. Y. Savrasov, G. Resta, X. Wan, Local Self-Energies for V and Pd Emergent from a Non-Local LDA+FLEX Implementation, *Phys. Rev. B* **97**, 155128 (2018).
- [21] H.-H. Lai, S. E. Grefe, S. Paschen, and Q. Si, Weyl-Kondo semimetal in heavy-fermion systems, *PNAS* **115**, 93 (2018).
- [22] I. Yang, S. Savrasov, and G. Kotliar, Importance of correlation effects on magnetic anisotropy in Fe and Ni, *Phys. Rev. Lett.* **87**, 216405 (2001).
- [23] A. A. Soluyanov, D. Gresch, Z. Wang, Q. Wu, M. Troyer, X. Dai and B. A. Bernevig, Type-II Weyl semimetals, *Nature* **527**, 495 (2015).
- [24] T.T.M. Palstra, G.J. Nieuwenhuys, R.F.M. Vlastuin, J. van den Berg, J.A. Mydosh, K.H.J. Buschow, Magnetic and electrical properties of several equiatomic ternary U-compounds, *J. Mag. and Magn. Mat.* **67**, 331 (1987).
- [25] Y. Du, E.-J. Kan, H. Xu, S. Y. Savrasov, X. Wan, Turning Copper Metal into Weyl Semimetal, *Phys. Rev. B* **97**, 245104 (2018).
- [26] X. Wan, A. M. Turner, A. Vishwanath, and S. Y. Savrasov, Topological semimetal and Fermi-arc surface states in the electronic structure of pyrochlore iridates, *Phys. Rev. B* **83**, 205101 (2011).
- [27] G. Resta, S.-T. Pi, X. Wan, S. Y. Savrasov, High Surface Conductivity of Fermi Arc Electrons in Weyl semimetals, *Phys. Rev. B* **97**, 085142 (2018).